ARMY RESEARCH LABORATORY

Computer Simulation of Soliton Interference Rejection Filter

Jeffrey Himmel and John Kosinski

ARL-TR-927 December 1995

NOTICES

Disclaimers

The findings in this report are not to be construed as an official Department of the Army position, unless so designated by other authorized documents.

The citation of trade names and names of manufacturers in this report is not to be construed as official Government endorsement or approval of commercial products or services referenced herein.

REPORT DOCUMENTATION PAGE

Form Approved
OMB NO. 0704-0188

1. AGENCY USE ONLY *(Leave blank)*	2. REPORT DATE	3. REPORT TYPE AND DATES COVERED
	December 1995	Final Report: Jul 95 to Nov 95

4. TITLE AND SUBTITLE
COMPUTER SIMULATION OF SOLITON INTERFERENCE REJECTION FILTER

5. FUNDING NUMBERS

6. AUTHOR(S)
Jeffrey Himmel and John Kosinski

7. PERFORMING ORGANIZATION NAMES(S) AND ADDRESS(ES)
US Army Research Laboratory (ARL)
Physical Sciences Directorate (PSD)
ATTN: AMSRL-PS-ED
Fort Monmouth, NJ 07703-5601

8. PERFORMING ORGANIZATION REPORT NUMBER
ARL-TR-927

9. SPONSORING / MONITORING AGENCY NAME(S) AND ADDRESS(ES)

10. SPONSORING / MONITORING AGENCY REPORT NUMBER

11. SUPPLEMENTARY NOTES

12a. DISTRIBUTION / AVAILABILITY STATEMENT
Approved for public release; distribution is unlimited.

12 b. DISTRIBUTION CODE

13. ABSTRACT *(Maximum 200 words)*

A soliton interference rejection filter which was recently proposed has been simulated with EEsof's Libra on a Sparc workstation. The filter depends on the use of solitons which are linearly independent in a nonlinear LC network. Such a filter would use the well-known sinusoidal recurrence phenomenon of solitons to separate, in time, a desired signal from a stronger undesired signal and conduct the undesired signal to ground at a specific location in the network. It was also suggested that the filter might change the harmonic content of only the undesired signal in order to decrease the amplitude of its fundamental. However, the computer simulations showed that multiple signals in a non-linear network do not become linearly independent solitons. It was also demonstrated that the ratio of the amplitudes of the desired and interfering fundamentals do not significantly change, regardless of what happens to the higher harmonics. The frequency and amplitude dependence of sinusoidal recurrence make it necessary to know a priori the frequencies and amplitudes of the incoming signals, which is unrealistic in a real communication system. Inter-modulation interference was also demonstrated. Thus, it was shown that a soliton interference rejection filter is not feasible.

14. SUBJECT TERMS
Soliton interference rejection filter; sinusoidal recurrence; solitons; nonlinear transmission line; nonlinear LC network; inter-modulation interference.

15. NUMBER IF PAGES
42

16. PRICE CODE

17. SECURITY CLASSIFICATION OR REPORT	18. SECURITY CLASSIFICATION OF THIS PAGE	19. SECURITY CLASSIFICATION OF ABSTRACT	20. LIMITATION OF ABSTRACT
Unclassified	Unclassified	Unclassified	UL

Contents

Figures

Tables

Introduction

A soliton interference rejection filter was recently proposed for the rejection of unwanted interference in communication applications [1]. This report discusses the computer simulation of such a filter in order to establish whether it would be feasible.

When a sinusoidal signal is introduced into a repetitive, nonlinear lumped LC network, i.e., a nonlinear transmission line, it changes its waveform as it progresses down the nonlinear transmission line. After some propagation distance called the "recurrence length," the sinusoidal waveform is restored, although not all of the energy is recovered in the fundamental frequency. This is known as the recurrence phenomenon. It can be explained by the existence in the nonlinear transmission line of stable nonlinear dispersive wave entities called "solitons," which have the following properties [2] [3].

1) A wave packet at any given position in the nonlinear LC network dissolves into multiple solitons.

2) Each soliton travels at a velocity which is directly proportional to its amplitude.

3) Solitons pass through each other without interacting, i.e., without losing their identities.

4) The number of solitons produced is proportional to the amplitude of the input sine wave.

The proposed rejection filter would make use of solitons which are linearly independent in a nonlinear transmission line. In other words, they wouldn't mix. The amplitude dependent velocity of the solitons would separate strong interference signals from weak desired signals. If this doesn't work, it was suggested that the soliton phenomenon could be used to change the harmonic content of an interfering signal in order to reduce the amplitude of its fundamental compared to the fundamental of a desired signal.

The feasibility of the soliton interference rejection filter was investigated by computer simulation on a Sparc workstation by using an EEsof software called Libra. The simulations used a harmonic balance algorithm. In order to proceed with the feasibility study, however, it was necessary to establish the ability of Libra to re-create experimental results which have been discussed in the literature. The experiments conducted by Fukushima (reference [3]) were found to be the most useful guideline for this purpose. The nonlinear transmission line described in reference [3] was modeled on Libra, and the experimental results which the authors obtained were re-created.

Once the reliability of Libra was established, two sinusoidal signals were fed into the computer model to test the ability of a nonlinear transmission line to filter out unwanted signals, as proposed.

Computer Simulation of Experimental Results Obtained by Fukushima

The nonlinear transmission line studied by Fukushima consisted of many sections. Each section consisted of a capacitor and inductor in parallel and a variable (nonlinear) capacitor, as shown in **Figure 1**. The values given by Fukushima for the inductor and capacitor were $L_1 = 31 \pm 2$ μH and $C_1 = 38 \pm 6$ pF, respectively. The variable capacitor which he used was voltage dependent and consisted of 2 diodes (Hitachi 1SV68) in parallel. At 6 volts, the variable capacitor had a capacitance of $C(6) = 40 \pm 4$ pF, and at 10 volts it had a capacitance of $C(10) = 26 \pm 3$ pF. The equation which describes the behavior of a variable capacitor was given by D. Jager [4] as

$$C(V) = C_0(1 - \delta V) \tag{1}$$

where C_0 and δ are constants. However, this can simplified into the equation form used by Libra, namely

$$C(V) = C_0 - KV, \tag{2}$$

where C_0 and K are constants, and $K = (\delta)(C_0)$. Fukushima's values for V and $C(V)$ were used to solve for the constants, yielding $C_0 = 61$ and $K = 3.5$. Thus, the behavior of the variable capacitor was described by $C(V) = 61 - 3.5V$.

Fukushima inserted a 1.429 MHz sinusoidal signal into various numbers of cascaded sections in order to find the recurrence length. This was modeled on Libra with a 50 Ω load resistor as illustrated in **Figure 2**. All measurements of the simulated output signal were measured across the load resistor. A 50 Ω signal source was represented as an AC voltage source cascaded with a 50 Ω resistor. The nonlinear network was purely reactive, i.e., it was reasonably assumed that it had negligible resistive losses. Thus, half of the voltage drop was across the source resistor and half across the load resistor.

The amplitude of Fukushima's input signal was 4 V. This was represented on Libra by providing an 8 volt signal and removing the nonlinear network, so that a 4 volt signal was fed directly into the load resistor, as illustrated in **Figure 3**. Using this configuration, the measurement of the input signal was simulated, as illustrated in **Figure 4**. Its Fourier transform is illustrated in **Figure 5**.

Fukushima illustrated the output wave forms resulting from using 13, 26, 39 and 52 LC cascaded sections, respectively. He used n to designate the number of sections. These experimental results are repeated here in **Figures 6** through **9**, where they are shown beside results which were simulated on Libra. Also shown in these figures are the Fourier transforms of the simulated waveforms. The computer simulations confirmed all the experimental results except when 26 sections were used. This one discrepancy can be

understood by the fact that in the real network constructed in the laboratory the components varied in value within some tolerances. Thus, the behavior of an ideal computer model will differ slightly from the real nonlinear network. Both Fukushima's experimental results and the simulated results agree that the recurrence length is 52 sections for a frequency of 1.429 MHz.

Fukushima defined the recurrence length n_R as the position along the nonlinear transmission line where the waveform *best coincided with the input waveform.* This definition indicates that he observed some distortion in the output sinusoidal signal when there was recurrence. Indeed, he superimposed the output signal at recurrence on top of the input signal (with the output signal normalized to the input signal) in order to show the distortion in the waveform, as is repeated here in **Figure 10**. In **Figure 9,** the Libra simulation for 52 sections shows that even at recurrence there was significant power in the higher harmonics, especially at the second harmonic. Thus, in the circuit simulations, the level of the second harmonic was used to distinguish between a very nearly sinusoidal output (recurrence) and a clearly nonsinusoidal output. The exact boundary was fuzzy. When the power of the second harmonic was less than about -16.0 dBc (compared with the fundamental) there was an apparent recurrence.

Table 1 indicates the bandwidth of recurrence for n = 52 sections. It also shows the power of the second harmonic both in units of dBm and dBc. The second to last column indicates the number of harmonics that were used in the harmonic balance simulation. The sinusoidal waveform recurred from 1.411 MHz to 1.432. This gave a recurrence bandwidth of 1.5%.

Fukushima calculated and experimentally determined the frequency dependence of the recurrence length for a 5 volt signal and a 9 volt signal. His theoretical and experimental results practically coincided. The experimental data are represented by open circles in **Figures 11** and **12**. Using his plots, the data points were tabulated as shown in **Table 2.** This frequency dependence was simulated on Libra. As shown in **Figure 11** and **Table 3**, the experimentally determined trends were re-created in the simulations for a 5 volt input signal. The simulations for a 9 volt input signal were extremely time consuming and memory intensive due to the significantly larger nonlinearity of a signal of this amplitude propagating down the nonlinear transmission line. Thus, there was only sufficient time to confirm the first data point of Fukushima. (See **Table 3** and **Figure 12.**) However, the general recurrence length trends observed and calculated by Fukushima were re-created in the simulations. Other recurrence lengths at other frequencies were also found in the simulations.

Clearly, the computer simulations of the experiments conducted by Fukushima yielded results which are in close agreement to his empirical results. Thus, the reliability of Libra to predict the behavior of a nonlinear transmission line has been established.

Simulation of Recurrence Power Range

The power range at which there is recurrence for 52 sections was simulated. The frequency of the input signal was 1.417 MHz. The input power was increased from 1 microwatt until the sine wave no longer recurred. It was found that there was recurrence for less than 0.3 watts. The results of these simulations are summarized in **Table 4**.

Inserting 2 Signals into the Nonlinear Transmission Line: Investigation of Inter-Modulation Interference

In order to investigate the ability of a nonlinear transmission line to filter out unwanted interference, it was necessary to simulate the insertion of two sinusoidal signals into the computer model. The weaker signal would represent the desired signal and the stronger signal would represent the interference at a particular frequency. Keep in mind that this greatly simplifies the problem, since the interference in a real communication system is often wideband noise. The frequencies chosen, 1.415 MHz and 1.423 MHz, were taken from the recurrence bandwidth of a nonlinear transmission line with 52 sections. The 1.415 MHz signal had a power of 1 mW and represented the desired signal. The 1.423 MHz signal was given a power level of 10 mW and represented interference.

A nonlinear element or network tends to mix the incoming signals. In a repetitive nonlinear network, as in this study, mixing products may themselves mix with each other as the signals propagate down the network. This intermixing of mixing products is called "inter-modulation interference." In order to test for this phenomenon, it was necessary to calculate the frequencies that would be produced by such mixing. This is shown in **Table 5**. **Table 5** also shows the expected mixing products that would occur without inter-modulation interference.

The input signals were first measured by removing the nonlinear transmission line and feeding the signals directly into the load resistor, as illustrated in **Figure 13**. The Fourier transform of this simulation is shown in **Figure 14**. All of the unwanted harmonics are shown at -270 dBm, the lower numerical limit of the software. In other words, this is how Libra shows that these harmonics don't exist in a linear element or system, such as a load resistor. Thus, as the signal propagates in the nonlinear transmission line, these harmonics must be significantly larger to be considered to exist.

The schematic for inserting the two signals into the nonlinear transmission line is illustrated in **Figure 15**. The number of sections was varied from 1 to 100. The Fourier transforms of these are illustrated in **Figures 16** to **23**. Inter-modulation interference was indeed observed in these figures. The power ratio of the two output signals is indicated in **Table 6** for different numbers of sections. The table also lists the power levels of two of the intermixing products. Notice that the undesired signal at 1.423 MHz was always a few dB higher than the desired signal (at 1.415 MHz).

As the number of sections increases, the network becomes more nonlinear. This requires a higher number of harmonics to be used in the harmonic balance algorithm of the software in order to retain a reasonable level of accuracy. (However, increasing the number of harmonics also increases the memory space required by the computer to do the calculations. For large nonlinear networks, the required memory space can easily exceed the available memory, so there is a trade-off.) For example, notice in **Table 6** that for $n = 100$ the power levels are different for different numbers of harmonics. However, even as the number of harmonics is increased to obtain a more reliable simulation, the interference signal is still higher in power than the desired signal.

Discussion: Comparison of Soliton Theory, the Proposal of a Soliton Filter and the Simulated Results

The recurrence phenomenon in nonlinear networks and the properties of solitons have been discussed in the literature. The recurrence phenomenon had been predicted theoretically and confirmed experimentally by Fukushima. Simulations using Libra decisively re-created the experimental results obtained by Fukushima. Thus, the reliability of Libra to predict the behavior of signals in a nonlinear transmission line has been conclusively established.

The proposal for a soliton interference rejection filter relies on the creation of solitons which are linearly independent in a nonlinear medium. The amplitude dependent velocity of the solitons would cause the solitons from an interference signal to be separated in time from the solitons of the desired signal. Each of the two signals would recur at different recurrence lengths. In other words, the solitons of each signal would catch up with each other to re-create the original sine wave at a specific location along the nonlinear transmission line. Thus, through a time gating scheme, the undesired signal would be tapped off at its recurrence length and conducted to ground, leaving only the desired signal. There are several problems with this idea.

One problem is that the recurrence phenomenon is frequency dependent. It is necessary to know *a priori* the frequencies of the interference signals in order to filter them out, assuming there is a clear separation in time of the desired and undesired solitons. This gets extremely complicated for more than two input signals. In addition, the simulations showed no clear time separation in solitons.

Another problem is the amplitude dependence of the recurrence phenomenon, as has been demonstrated experimentally by Fukushima and simulated on Libra (**Figures 11** and **12** and **Table 4**). This amplitude dependence creates the requirement of knowing *a priori* the amplitudes of the multiple signals received by an antenna in a communication system. However, it is impossible to predict the signal amplitudes. The power of the transmitting station is usually unknown. The power of the received signal depends on the distance of the transmitting station from the receiver, and this is often unknown, especially if the transmitting and receiving stations are moving. Also, the power of

signals change in time drastically due to unpredictable environmental factors. Those environmental factors are particularly unpredictable in a combat situation.

The simulations involving two signals demonstrated that multiple signals do not become linearly independent solitons. The signals mix. Thus, there is no linear superposition of multiple signals in a nonlinear system.

In addition to ordinary mixing, the computer simulations demonstrated the existence of inter-modulation interference for two signals propagating down a large nonlinear network. The increased mixing products complicates the task of filtering, especially with numerous input signals.

When two or more signals propagate down the nonlinear network, there is no significant change in the difference between the amplitudes of the desired and undesired signals. The signal that is higher in amplitude remains higher in amplitude. The energy of the fundamentals of both the desired and undesired signals is transferred to higher harmonics. Thus, the nonlinear transmission line does not filter out the undesired signal by transferring exclusively its energy to higher harmonics. There is a gradual change in the relative amplitudes of the fundamentals of the two signals. However, these changes occur extremely slowly as the number of sections increases. If there is a number of sections that can eventually significantly change the relative amplitudes of the two fundamentals, that number of sections would be much too huge to be practical.

The results of the simulations indicate that a soliton interference rejection filter would not be a practical way of filtering out unwanted noise.

References

[1] Stuart D. Albert, "A Possible Application of Solitons Propagating on a Nonlinear Transmission Line to Interference Reduction," to be published as a Technical Report, U.S. Army Research Laboratory, Physical Sciences Directorate.

[2] Ryogo Hirota and Kimio Suzuki, "Theoretical and Experimental Studies of Lattice Solitons in Nonlinear Lumped Networks," Proceedings of the IEEE, Vol. 61, No. 10, October 1973.

[3] Kazuhiro Fukushima, Miki Wadati, Takeyasu Kotera, Katsuro Sawada and Yoshimasa Narahara, "Experimental and Theoretical Study of the Recurrence Phenomena in Nonlinear Transmission Line," Journal of the Physical Society of Japan, Vol. 48, No. 3, March 1980.

[4] D. Jager, "Soliton Propagation along Periodic-Loaded Transmission Line," Institut für Angewandte Physik, Universität, D-4400 Münster, Fed. Rep. Germany, 3 January 1978.

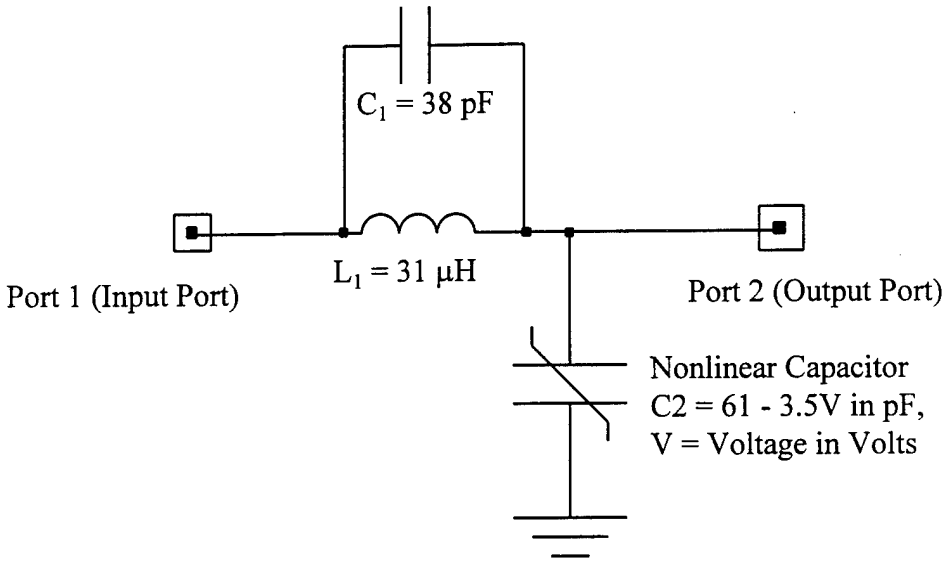

Figure 1: One section of the nonlinear transmission line.

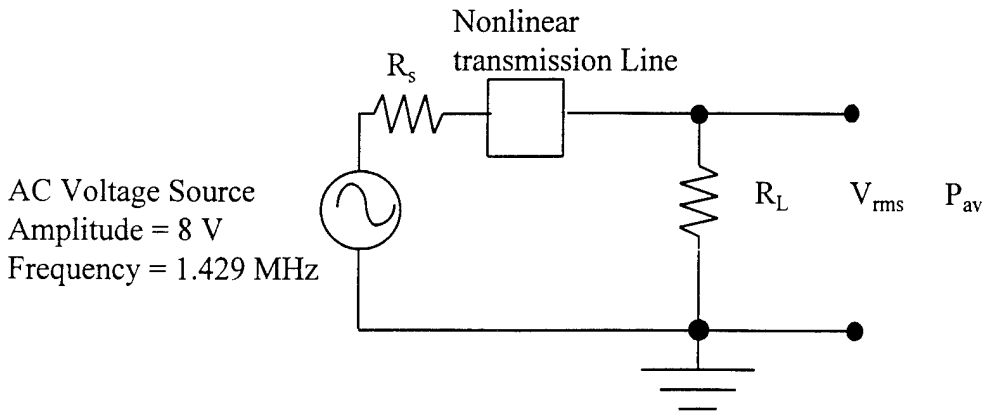

$R_s = R_L = 50\ \Omega$

Figure 2: Simulated test setup for inserting one sinusoidal signal into the nonlinear transmission line. The nonlinear transmission line may consist of numerous cascaded LC sections. The root mean square output voltage V_{rms} and the average power output P_{av} was measured across the load resistor R_L.

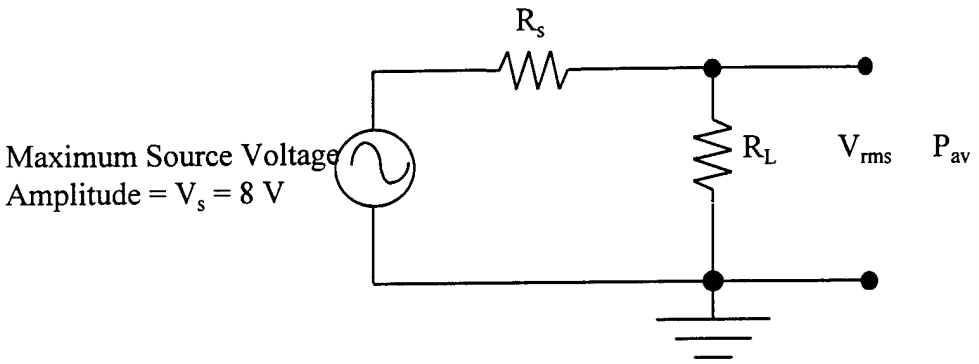

$R_s = R_L = 50$ ohms

Input Power = $P_{av} = V_{rms}^2 / R_L$

$V_{rms} = [P_{av} R_L]^{1/2}$

$V_s = 2[2]^{1/2} V_{rms}$

Figure 3: Computer model with which the time domain and Fourier transform of the input signal was simulated.

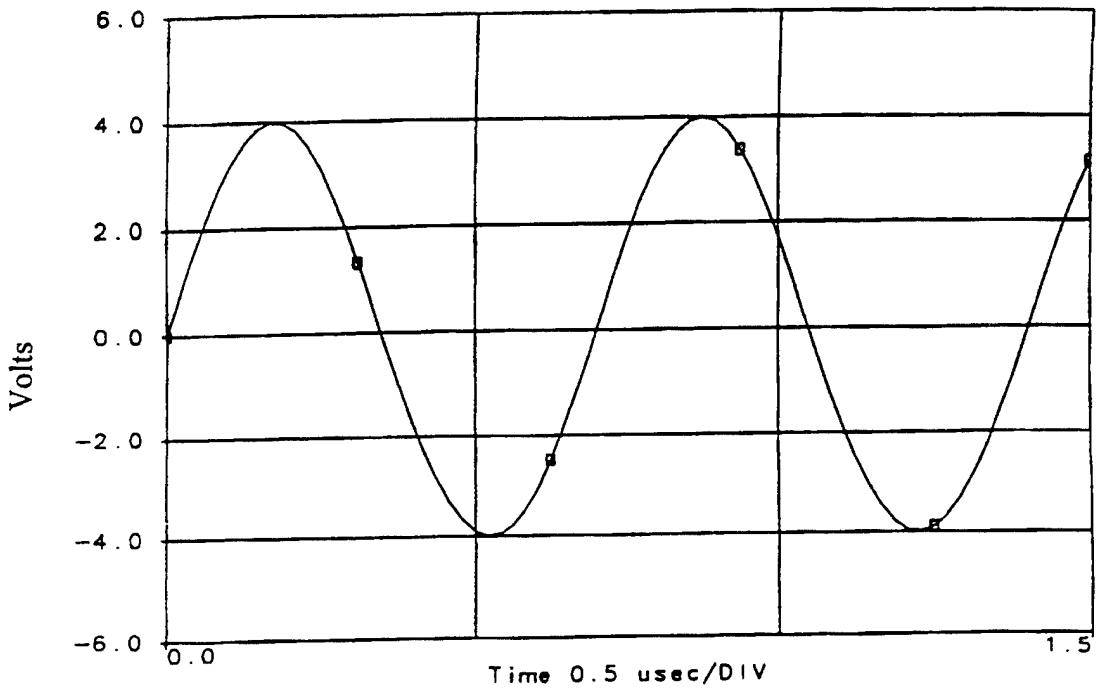

Number of Harmonics = 11
Frequency = 1.429 MHz

Figure 4: Simulated waveform of input signal.

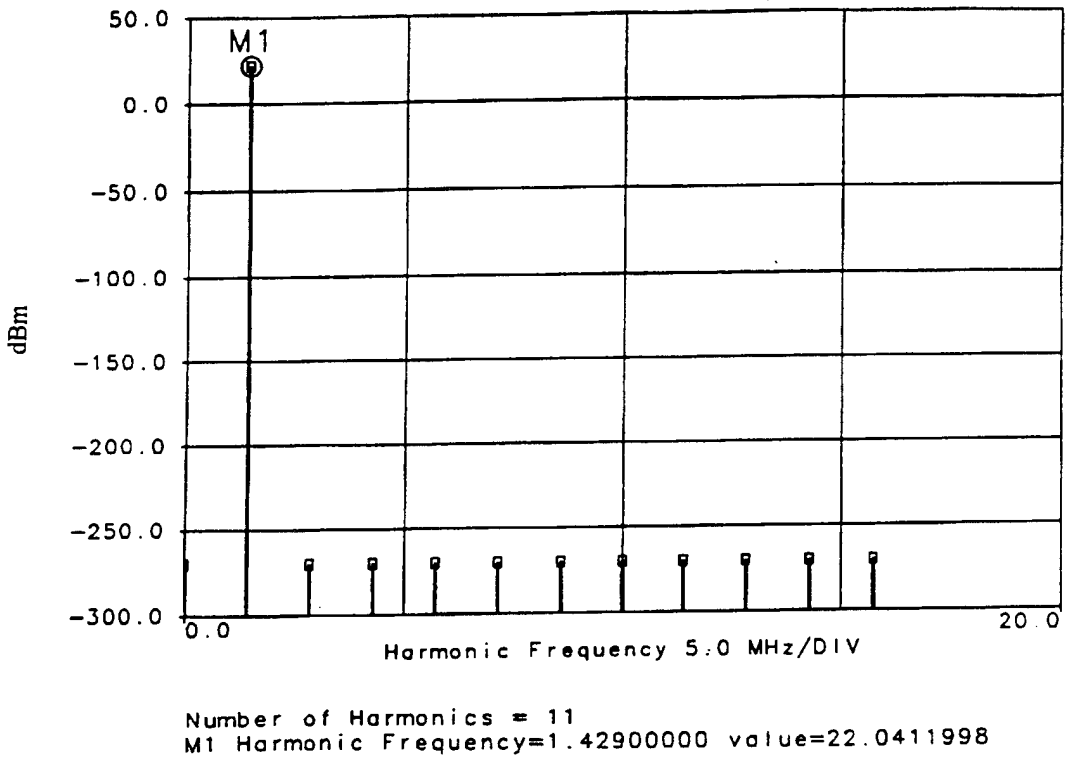

Figure 5: Fourier transform of simulated input signal. Note that the marker is designated as "M1" and given a value in dBm.

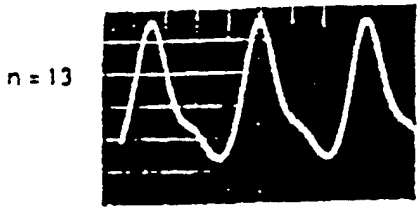

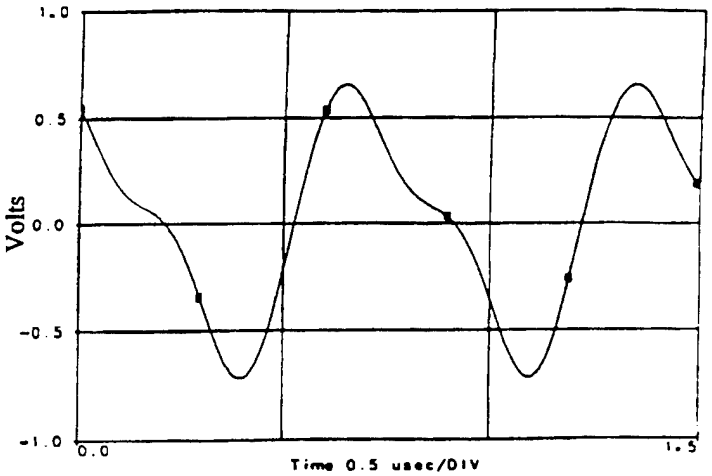

Number of Harmonics = 11 Number of LC Sections = 13
Frequency = 1.429 MHz

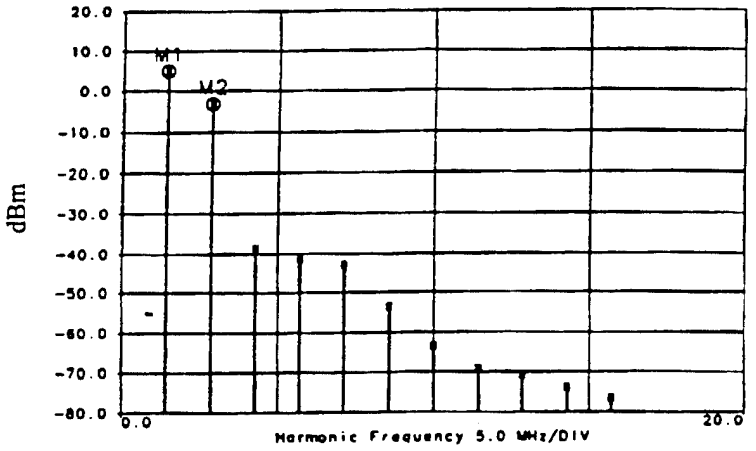

Number of Harmonics = 11 Number of LC Sections = 13
M1 Harmonic Frequency = 1.42900000 value = 5.13625746
M2 Harmonic Frequency = 2.85800000 value = -3.22183735

Figure 6: Output signal waveform for n = 13 sections. At top left is the experimental result obtained by Fukushima. The oscilloscope settings were 2 volts/division for the ordinate and 0.2 μsec/division for the abscissa. At top right is the waveform simulated on Libra. At bottom is the Fourier transform of the Libra simulation. The values of the markers are in dBm.

n = 26

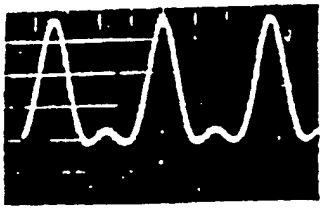

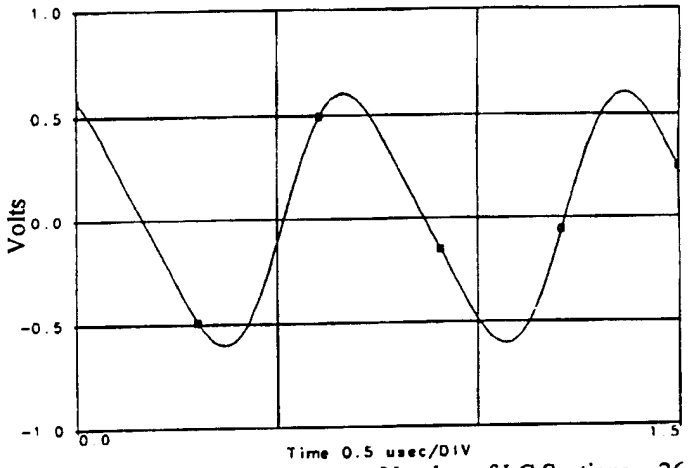

Number of Harmonics = 6 Number of LC Sections = 26
Frequency = 1.429 MHz

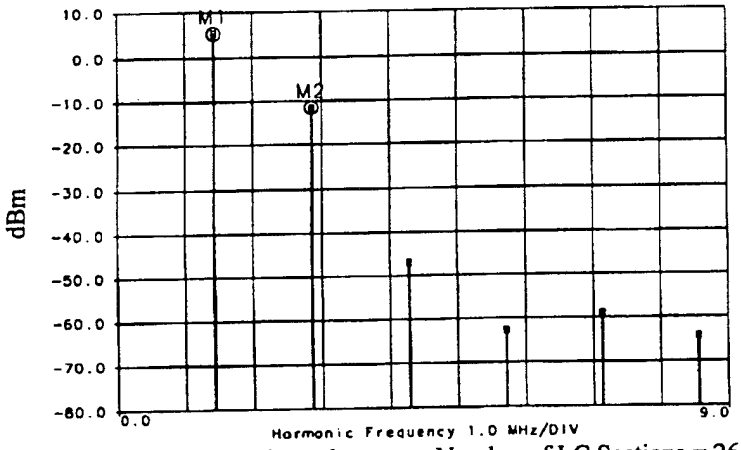

Number of Harmonics = 6 Number of LC Sections = 26
M1 Harmonic Frequency = 1.42900000 value = 5.28508882
M2 Harmonic Frequency = 2.85800000 value = -11.5546819

Figure 7: Output signal waveform for n = 26 sections. At top left is the experimental result obtained by Fukushima. The oscilloscope settings were 2 volts/division for the ordinate and 0.2 μsec/division for the abscissa. At top right is the waveform simulated on Libra. At bottom is the Fourier transform of the Libra simulation. The values of the markers are in dBm.

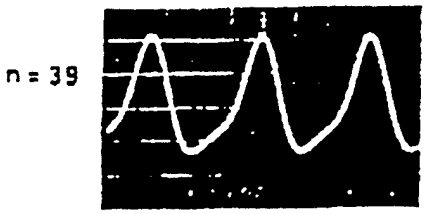

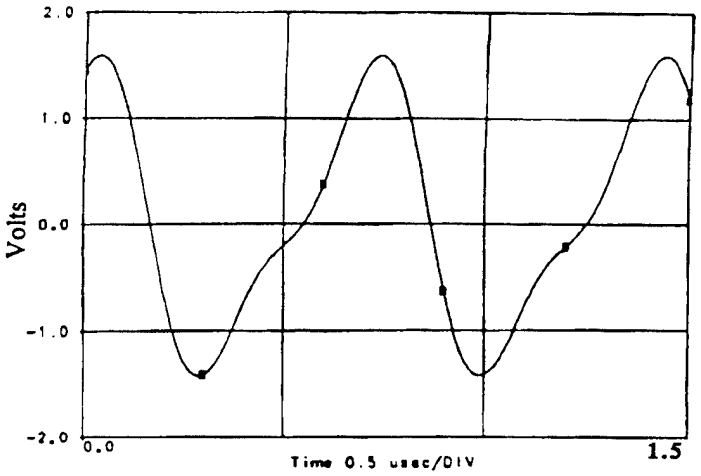

Number of Harmonics = 6 Number of LC Sections = 39
Frequency = 1.429 MHz

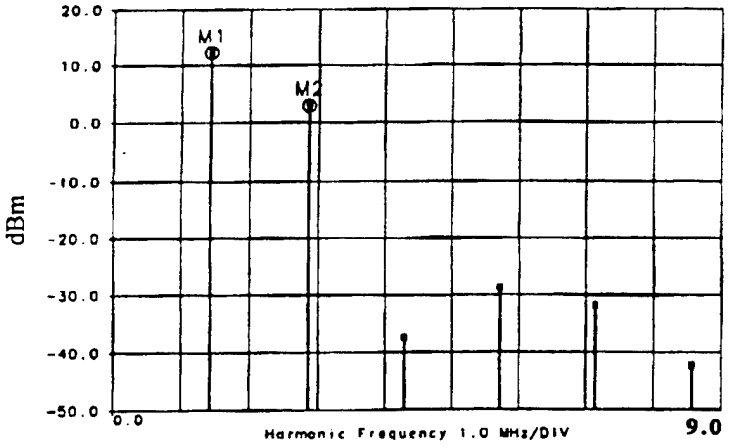

Number of Harmonics = 6 Number of LC Sections = 39
M1 Harmonic Frequency = 1.42900000 value = 12.3526714
M2 Harmonic Frequency = 2.85800000 value = 2.93947590

Figure 8: Output signal waveform for n = 39 sections. At top left is the experimental result obtained by Fukushima. The oscilloscope settings were 2 volts/division for the ordinate and 0.2 μsec/division for the abscissa. At top right is the waveform simulated on Libra. At bottom is the Fourier transform of the Libra simulation. The values of the markers are in dBm.

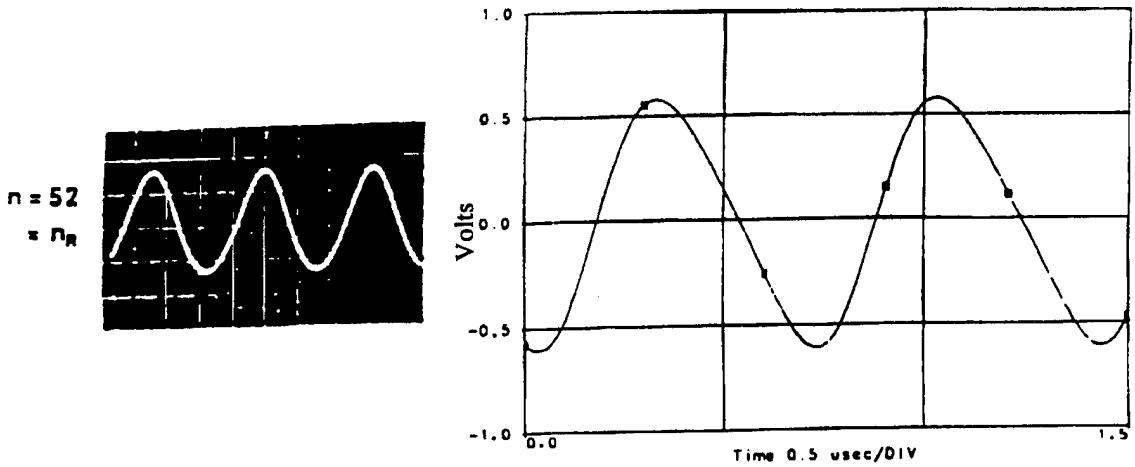

Number of Harmonics = 11 Number of LC Sections = 52
Frequency = 1.429 MHz

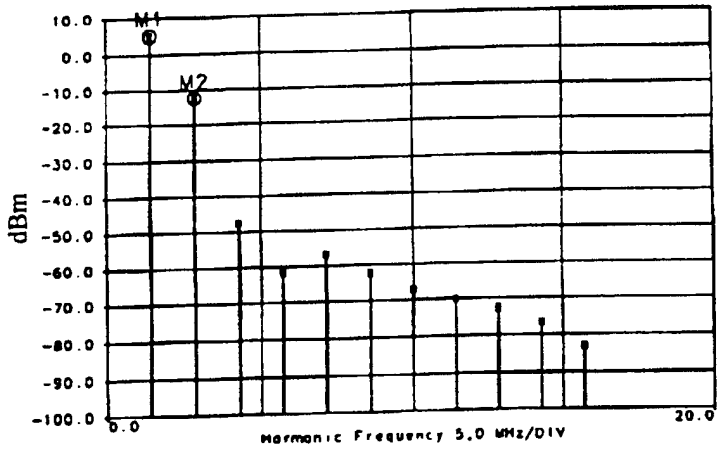

Number of Harmonics = 11 Number of LC Sections = 52
M1 Harmonic Frequency = 1.42900000 value = 5.22076961
M2 Harmonic Frequency = 2.85800000 value = -12.3243704

Figure 9: Output signal waveform for n = 52 sections. At top left is the experimental result obtained by Fukushima. The oscilloscope settings were 2 volts/division for the ordinate and 0.2 μsec/division for the abscissa. At top right is the waveform simulated on Libra. At bottom is the Fourier transform of the Libra simulation. The values of the markers are in dBm. Notice that the sinusoidal recurrence length n_R is 52 sections for 1.429 MHz.

$n = 0$
and
$n = n_R$

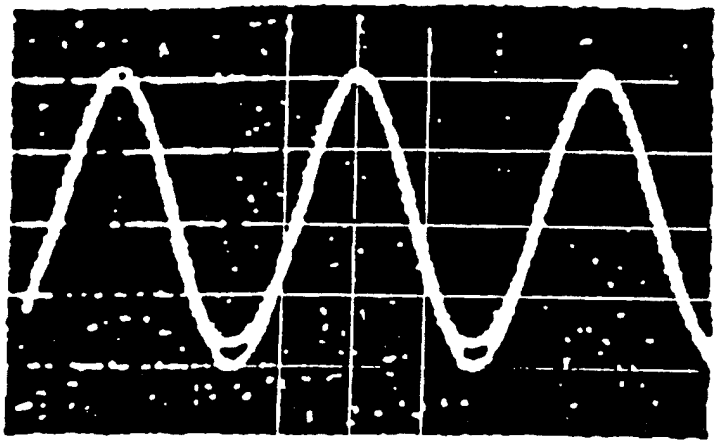

Figure 10: Fukushima's output signal at recurrence superimposed on the input signal. The recurrence length was $n_R = 52$. The output signal was normalized to the input signal.

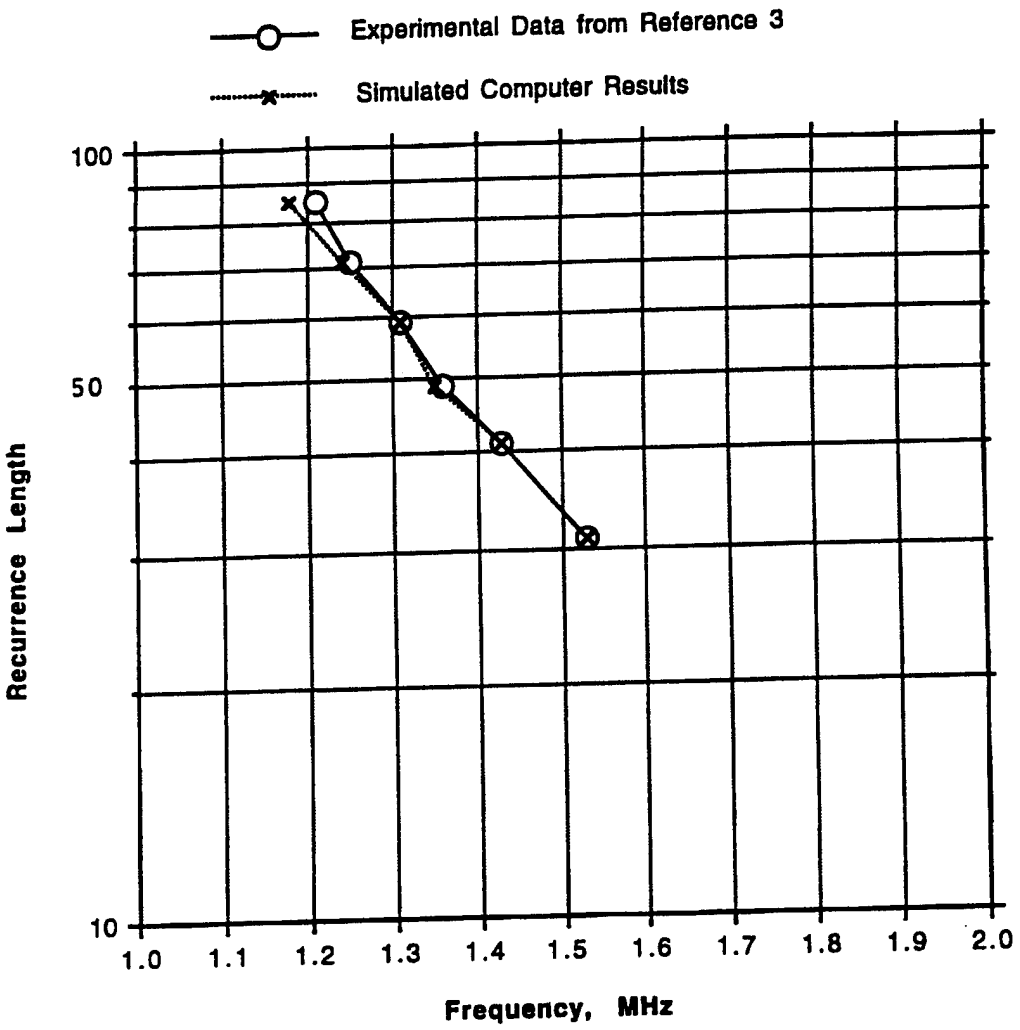

Figure 11: Frequency dependence of the recurrence length for an input signal with a 5 volt amplitude. Experimental data from reference 3 are compared to simulated computer results.

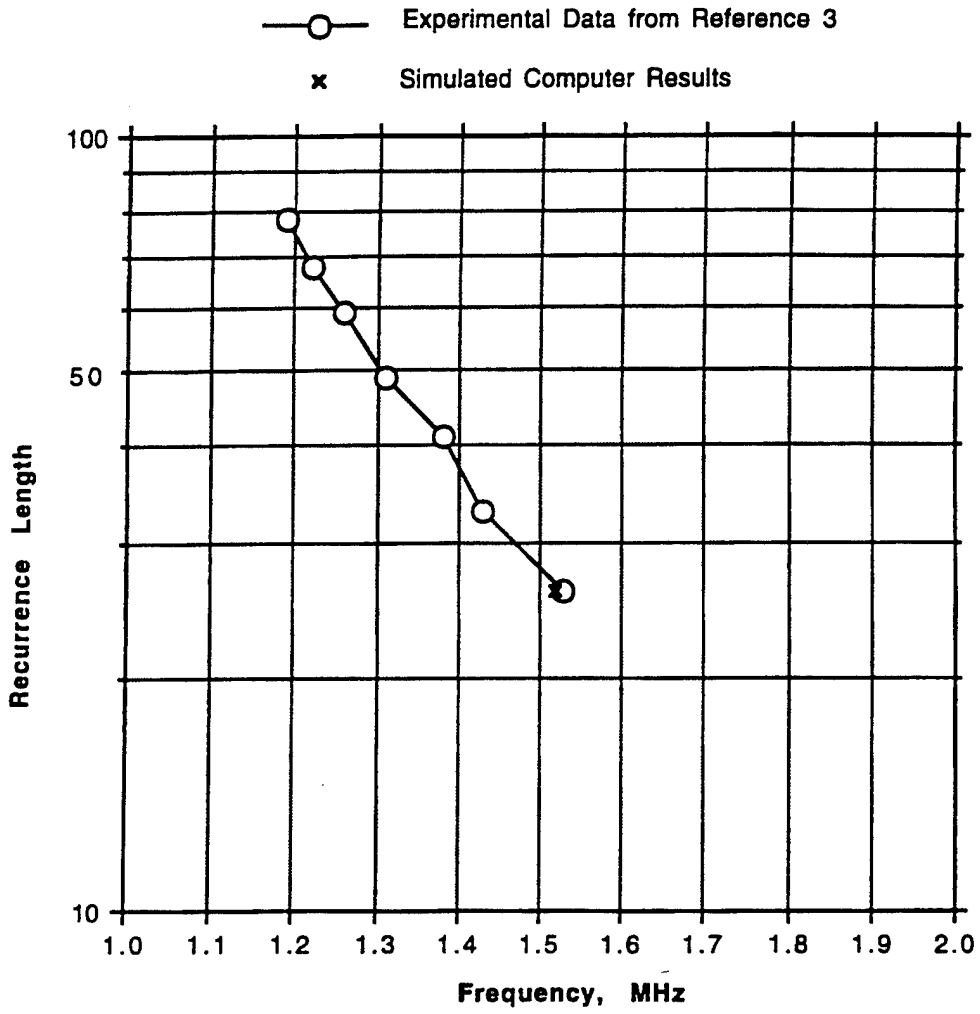

Figure 12: Frequency dependence of the recurrence length for an input signal with a 9 volt amplitude. Experimental data from reference 3 are compared to simulated computer results.

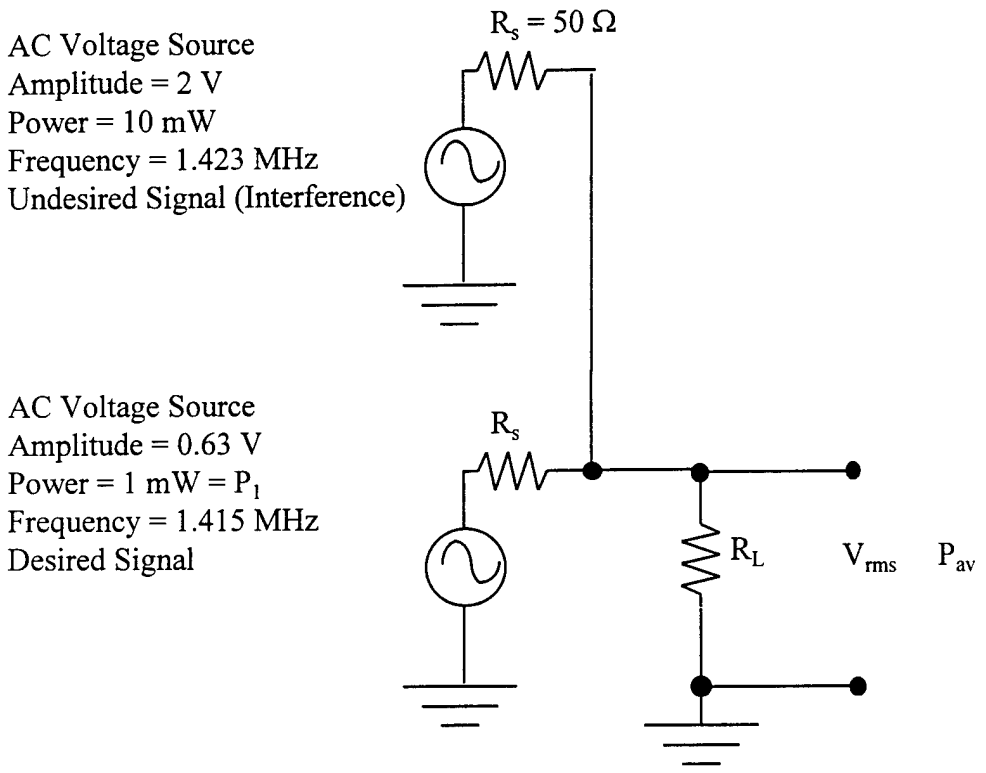

Figure 13: Schematic for simulation of measuring two input sinusoidal signals. The two signals were inserted simultaneously into the load resistor $R_L = 50\ \Omega$.

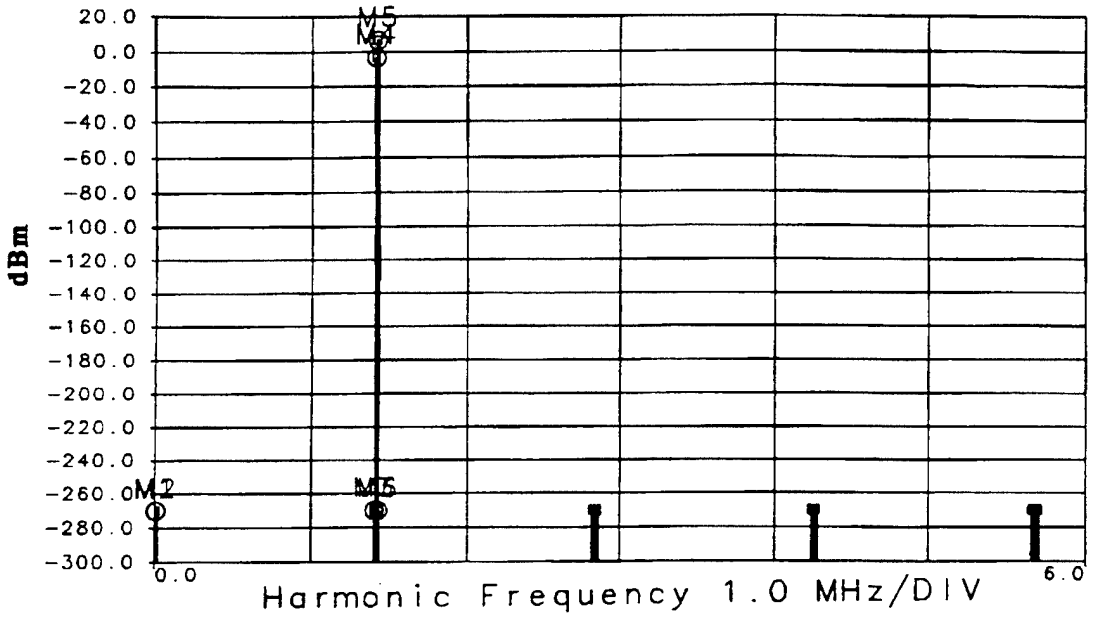


```
_freq1 = 1.415 MHz          _freq2 = 1.423 MHz
Number of Harmonics: 4
M1 Harmonic Frequency=0.00800000 value=-270.000000
M2 Harmonic Frequency=0.01600000 value=-270.000000
M3 Harmonic Frequency=1.40700000 value=-270.000000
M4 Harmonic Frequency=1.41500000 value=-3.52808353
M5 Harmonic Frequency=1.42300000 value=6.47817482
M6 Harmonic Frequency=1.43100000 value=-270.000000
```

Figure 14: Simulated Fourier transform of the two input signals that were fed into the nonlinear transmission line models.

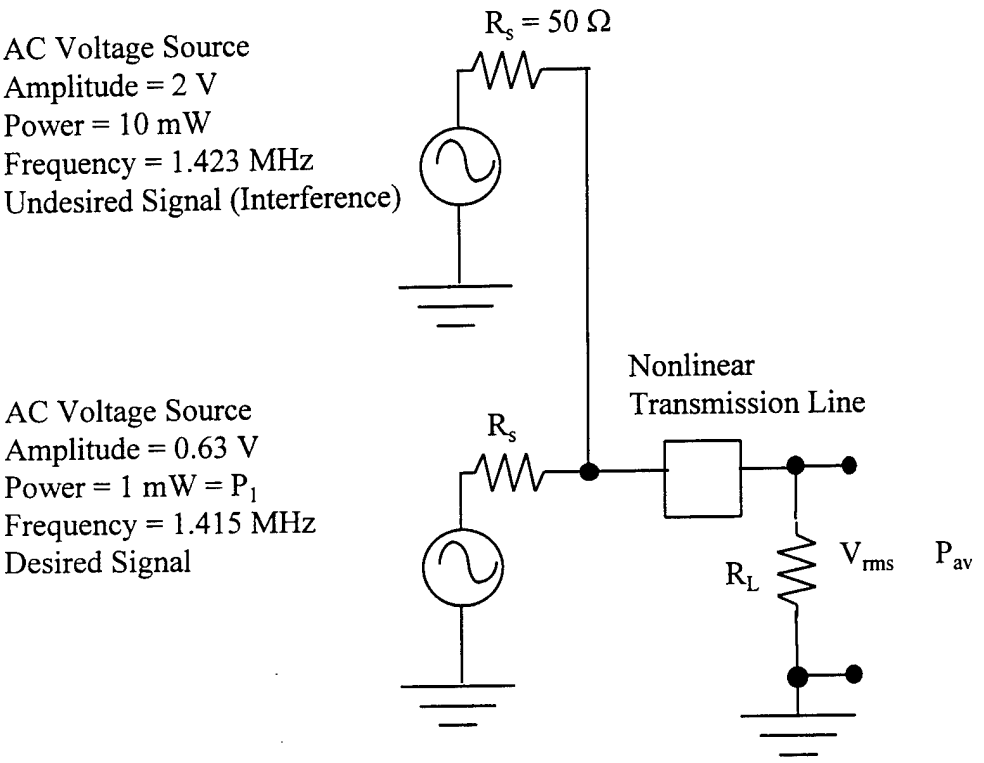

Figure 15: Schematic for inserting two input sinusoidal signals into a nonlinear transmission line. The load resistor was $R_L = 50\ \Omega$.

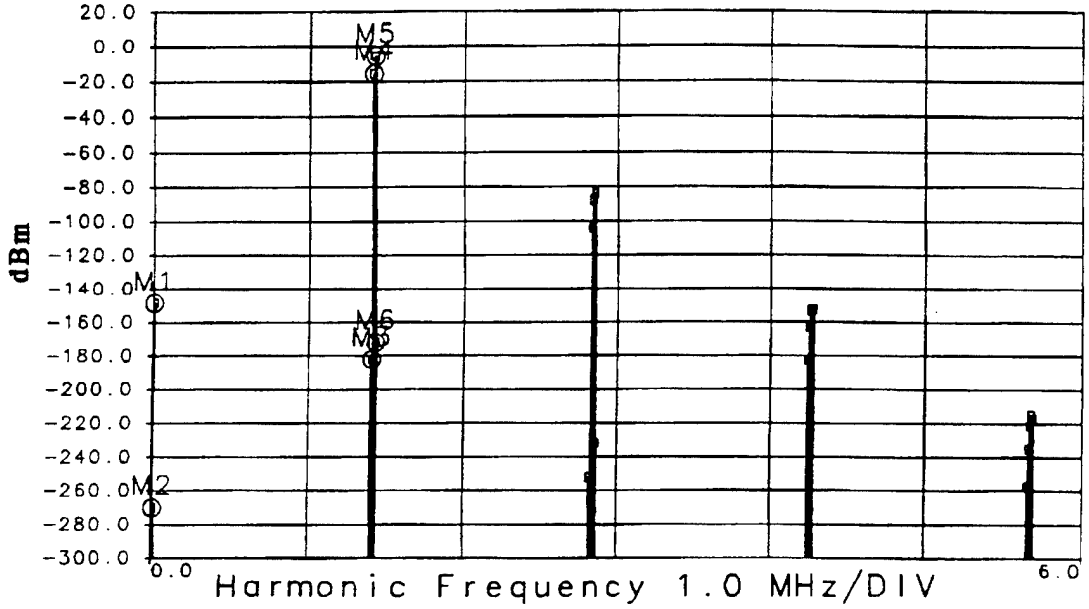


```
_freq1 = 1.415 MHz                    _freq2 = 1.423 MHz
Number of Sections: 1    Number of Harmonics: 4
M1 Harmonic Frequency=0.00800000 value=-148.427394
M2 Harmonic Frequency=0.01600000 value=-270.000000
M3 Harmonic Frequency=1.40700000 value=-182.215403
M4 Harmonic Frequency=1.41500000 value=-15.9048980
M5 Harmonic Frequency=1.42300000 value=-5.95440814
M6 Harmonic Frequency=1.43100000 value=-172.027169
```

Figure 16: Simulation of output mixing products resulting from feeding two sinusoidal signals into a nonlinear network with 1 LC section.

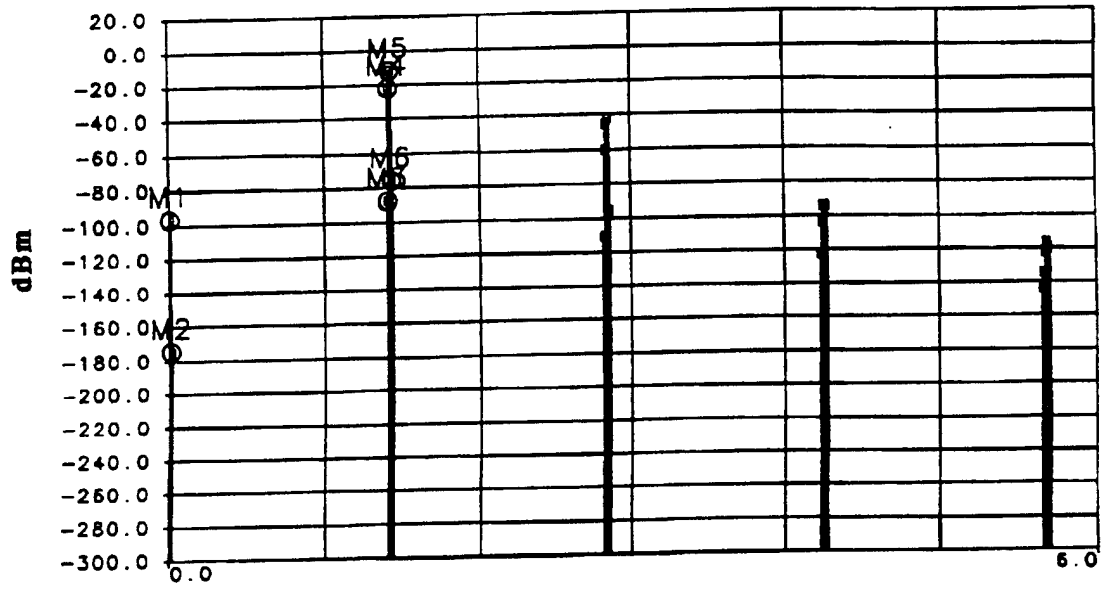


```
_freq1 = 1.415 MHz                    _freq2 = 1.423 MHz
Number of Sections: 13  Number of Harmonics: 4
M1 Harmonic Frequency=0.00800000 value=-96.2570081
M2 Harmonic Frequency=0.01600000 value=-174.085970
M3 Harmonic Frequency=1.40700000 value=-87.5398538
M4 Harmonic Frequency=1.41500000 value=-22.0879830
M5 Harmonic Frequency=1.42300000 value=-11.8716654
M6 Harmonic Frequency=1.43100000 value=-75.7948826
```

Figure 17: Simulation of output mixing products resulting from feeding two sinusoidal signals into a nonlinear network with 13 LC sections.

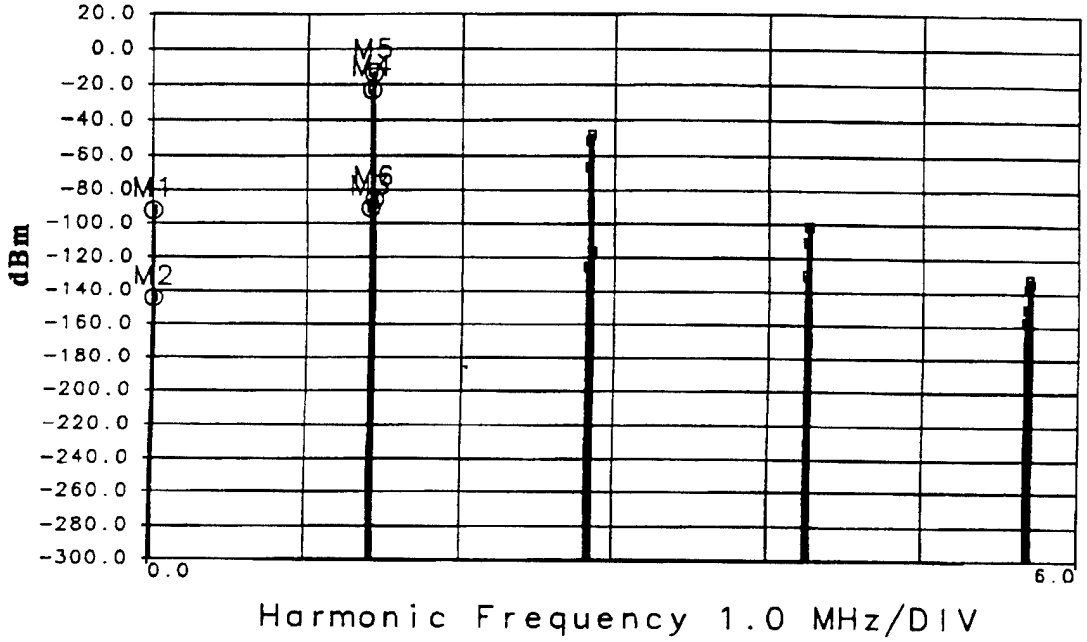


```
_freq1 = 1.415 MHz                    _freq2 = 1.423 MHz
Number of Sections: 26  Number of Harmonics: 4
M1 Harmonic Frequency=0.00800000 value=-92.5369504
M2 Harmonic Frequency=0.01600000 value=-144.683635
M3 Harmonic Frequency=1.40700000 value=-90.9846177
M4 Harmonic Frequency=1.41500000 value=-23.1053111
M5 Harmonic Frequency=1.42300000 value=-13.3157307
M6 Harmonic Frequency=1.43100000 value=-85.8641982
```

Figure 18: Simulation of output mixing products resulting from feeding two sinusoidal signals into a nonlinear network with 26 LC sections.

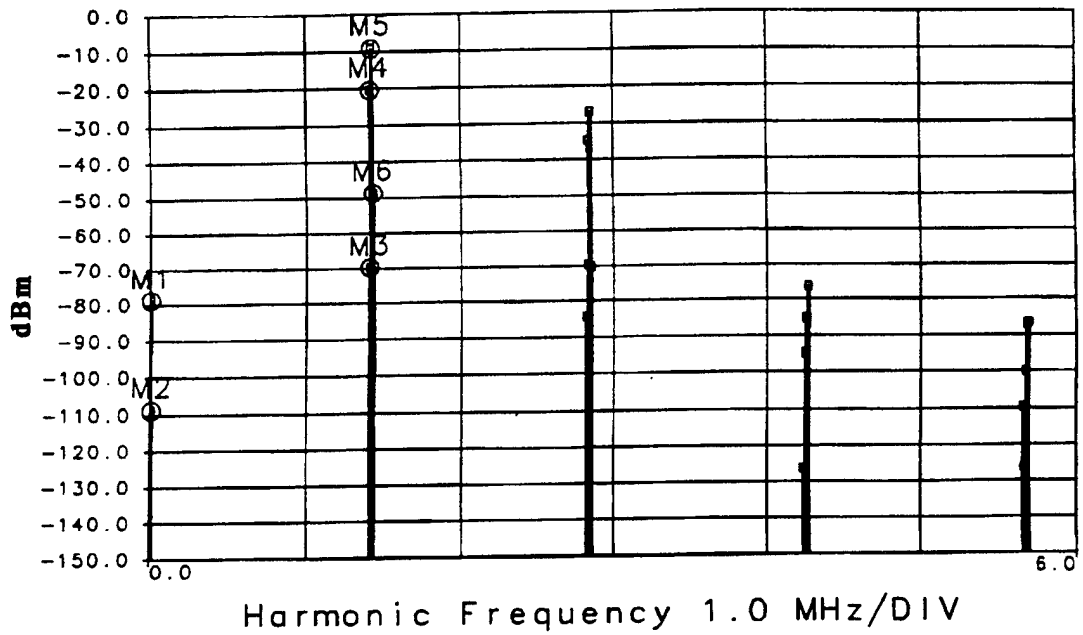


```
_freq1 = 1.415 MHz                    _freq2 = 1.423 MHz
Number of Sections: 52   Number of Harmonics = 4
M1 Harmonic Frequency=0.00800000 value=-78.7291922
M2 Harmonic Frequency=0.01600000 value=-108.790150
M3 Harmonic Frequency=1.40700000 value=-69.7620713
M4 Harmonic Frequency=1.41500000 value=-20.5291050
M5 Harmonic Frequency=1.42300000 value=-9.11734961
M6 Harmonic Frequency=1.43100000 value=-48.7993138
```

Figure 19: Simulation of output mixing products resulting from feeding two sinusoidal signals into a nonlinear network with 52 LC sections.

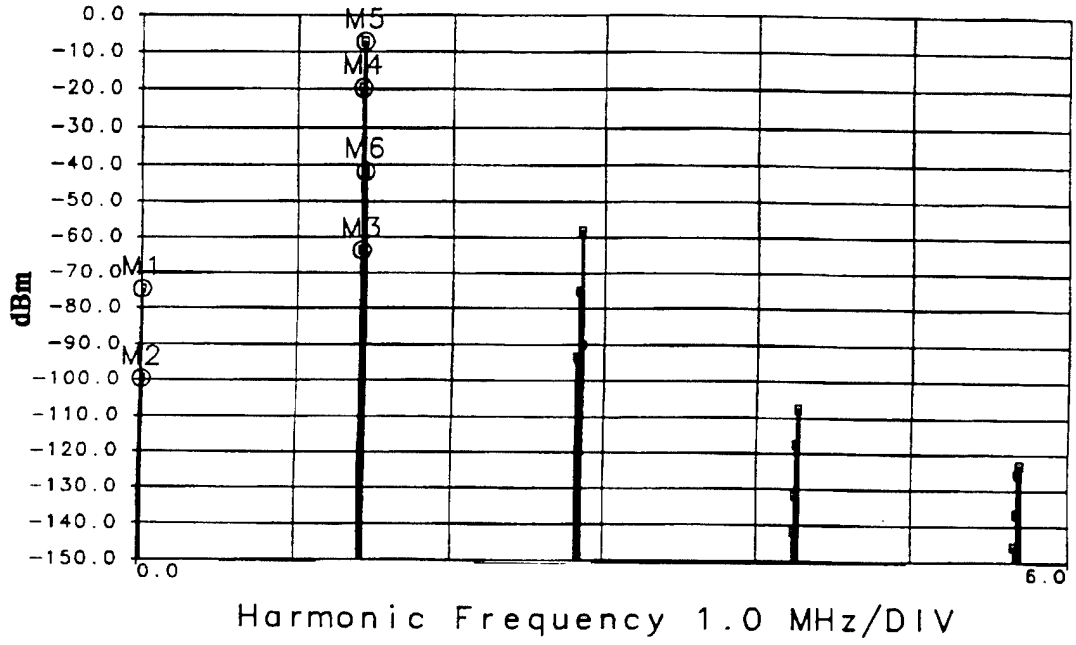


```
_freq1 = 1.415 MHz                    _freq2 = 1.423 MHz
Number of Sections: 60   Number of Harmonics = 4
M1 Harmonic Frequency=0.00800000 value=-74.5354587
M2 Harmonic Frequency=0.01600000 value=-99.7550797
M3 Harmonic Frequency=1.40700000 value=-63.6280398
M4 Harmonic Frequency=1.41500000 value=-19.5887474
M5 Harmonic Frequency=1.42300000 value=-7.18605341
M6 Harmonic Frequency=1.43100000 value=-41.7800448
```

Figure 20: Simulation of output mixing products resulting from feeding two sinusoidal signals into a nonlinear network with 60 LC sections.

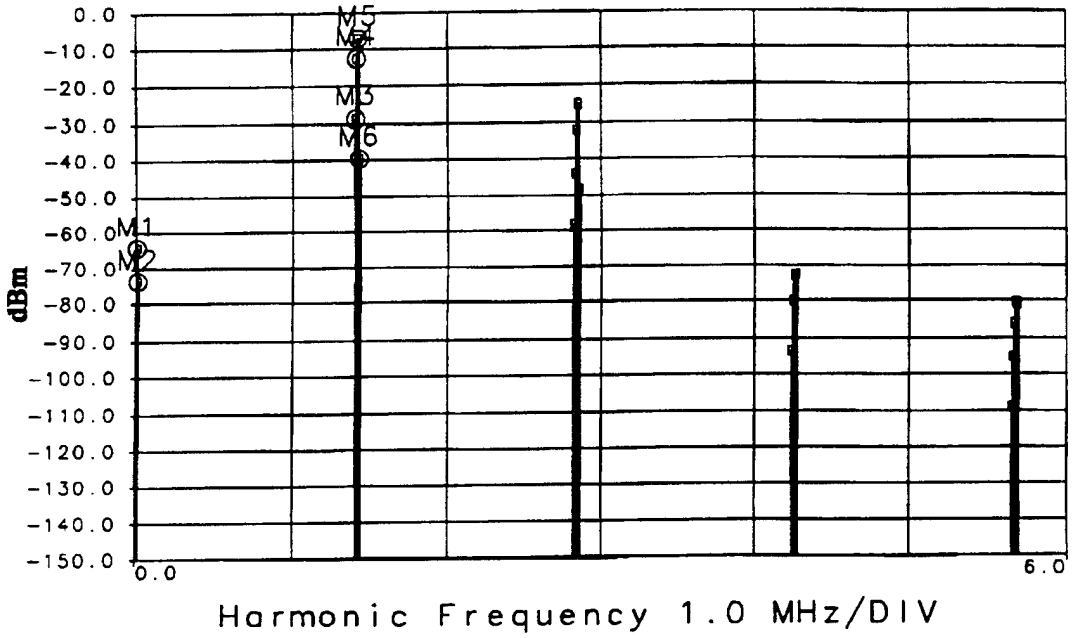


```
_freq1 = 1.415 MHz                    _freq2 = 1.423 MHz
Number of Sections: 70    Number of Harmonics = 4
M1 Harmonic Frequency=0.00800000 value=-64.1907516
M2 Harmonic Frequency=0.01600000 value=-73.6028215
M3 Harmonic Frequency=1.40700000 value=-28.7031758
M4 Harmonic Frequency=1.41500000 value=-12.6065806
M5 Harmonic Frequency=1.42300000 value=-7.06301384
M6 Harmonic Frequency=1.43100000 value=-39.5986711
```

Figure 21: Simulation of output mixing products resulting from feeding two sinusoidal signals into a nonlinear network with 70 LC sections.

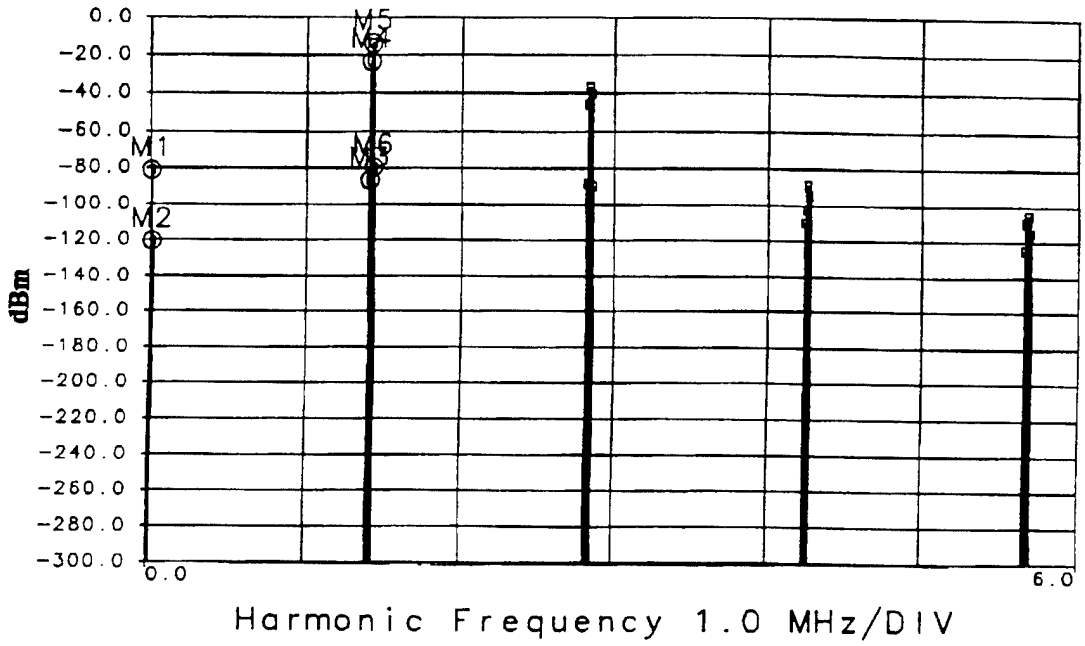

_freq1 = 1.415 MHz _freq2 = 1.423 MHz
Number of Sections: 80 Number of Harmonics = 4

```
M1 Harmonic Frequency=0.00800000 value=-81.2721849
M2 Harmonic Frequency=0.01600000 value=-120.462920
M3 Harmonic Frequency=1.40700000 value=-86.7425931
M4 Harmonic Frequency=1.41500000 value=-23.3312047
M5 Harmonic Frequency=1.42300000 value=-13.6871001
M6 Harmonic Frequency=1.43100000 value=-79.7338118
```

Figure 22: Simulation of output mixing products resulting from feeding two sinusoidal signals into a nonlinear network with 80 LC sections.

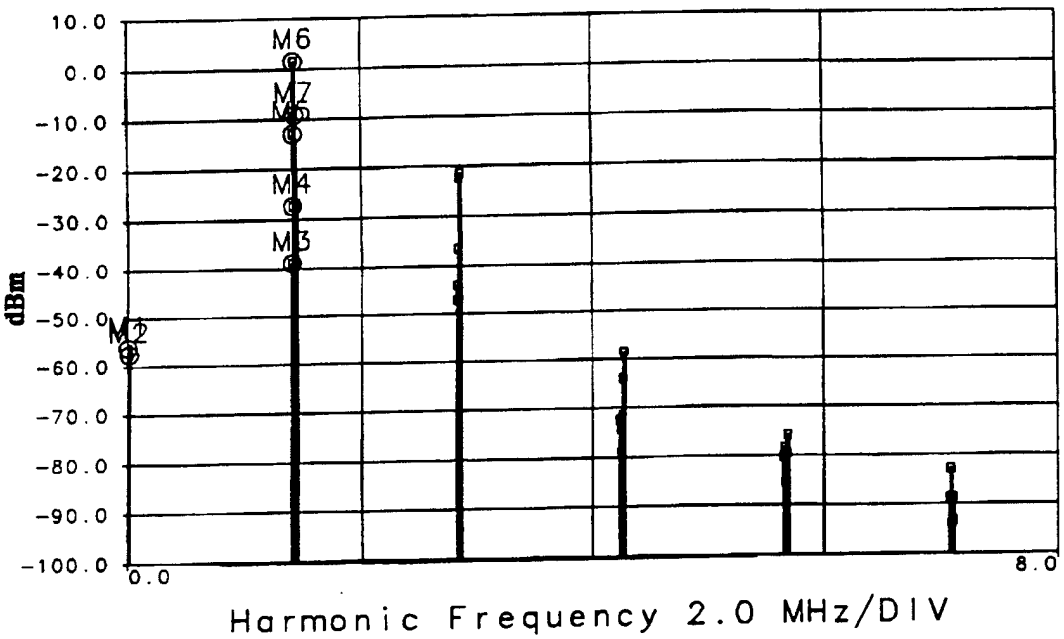

_freq1 = 1.415 MHz _freq2 = 1.423 MHz
Number of Sections: 100 Number of Harmonics = 5
M1 Harmonic Frequency=0.00800000 value=-56.1512424
M2 Harmonic Frequency=0.01600000 value=-57.4546187
M3 Harmonic Frequency=1.39900000 value=-38.8550213
M4 Harmonic Frequency=1.40700000 value=-27.3920124
M5 Harmonic Frequency=1.41500000 value=-12.9937211
M6 Harmonic Frequency=1.42300000 value=1.48863648
M7 Harmonic Frequency=1.43100000 value=-9.23542089

Figure 23: Simulation of output mixing products resulting from feeding two sinusoidal signals into a nonlinear network with 100 LC sections.

Table 1: Recurrence bandwidth for n = 52 LC sections.

Note: Number of harmonics used in the harmonic balance simulation is designated by NH.

Test Frequency vs. Recurrence Length						
First Harmonic		Second Harmonic				
Frequency, MHz	**Power, dBm**	**Frequency, MHz**	**Power, dBm**	**Power, dBc**	**NH**	**Comments**
1.410	4.5	2.820	-11.4	-15.9	11	nonsinusoidal
1.411	4.6	2.822	-11.7	-16.3	11	sinusoidal
1.413	4.6	2.826	-12.2	-16.8	11	sinusoidal
1.414	4.7	2.828	-12.4	-17.1	11	sinusoidal
1.416	4.7	2.832	-12.8	-17.5	11	sinusoidal
1.417	4.8	2.834	-13.0	-17.8	11	sinusoidal
1.418	4.8	2.836	-13.1	-17.9	11	sinusoidal
1.419	4.8	2.838	-13.3	-18.1	11	sinusoidal
1.420	4.9	2.840	-13.4	-18.3	11	sinusoidal
1.421	4.9	2.842	-13.5	-18.4	11	sinusoidal
1.422	4.9	2.844	-13.5	-18.4	11	sinusoidal
1.423	5.0	2.846	-13.5	-18.5	11	sinusoidal
1.424	5.0	2.848	-13.5	-18.5	11	sinusoidal
1.425	5.1	2.850	-13.4	-18.5	11	sinusoidal
1.426	5.1	2.852	-13.2	-18.3	11	sinusoidal
1.427	5.1	2.854	-13.0	-18.1	11	sinusoidal
1.428	5.2	2.856	-12.7	-17.9	11	sinusoidal
1.429	5.2	2.858	-12.3	-17.5	11	sinusoidal
1.432	5.7	2.864	-11.3	-17.0	11	sinusoidal
1.433	5.3	2.866	-9.3	-14.6	11	nonsinusoidal

Bandwidth = BW = (1.432 - 1.411) MHz = 0.021 MHz

Normalized to bandwidth center:

$$BW = \frac{0.021\ \text{MHz}}{1.422\ \text{MHz}} 100 = 1.5\ \%$$

Table 2: Data taken from Fukushima's plots of frequency versus recurrence length.

Key:

n_R = Number of LC sections (recurrence length)
f = Recurrence frequency in MHz
A = Input signal amplitude in volts

n_R	f	A
31	1.53	5
41	1.43	5
49	1.36	5
59	1.31	5
71	1.25	5
85	1.21	5
26	1.53	9
33	1.43	9
41	1.38	9
49	1.31	9
59	1.26	9
68	1.22	9
78	1.19	9

Table 3: Simulated test frequency versus recurrence length.

Key:
n_R = Recurrence length
f_1 = Fundamental frequency
P_1 = Power of the fundamental
f_2 = Second harmonic
P_2 = Power of second harmonic
NH = Number of harmonics used in simulation

Amplitude (volts)	**n_R**	**f_1 (MHz)**	**P_1 (dBm)**	**f_2 (MHz)**	**P_2 (dBm)**	**P_2 (dBc)**	**NH**
5	31	1.50	2.8	3.00	-22.3	-25.1	12
5	31	1.51	1.9	3.02	-25.4	-27.3	12
5	31	1.52	1.2	3.04	-22.6	-23.8	12
5	31	1.53	0.7	3.06	-19.9	-20.6	12
5	31	1.54	0.4	3.08	-16.0	-16.4	12
5	41	1.41	3.4	2.82	-17.0	-20.4	12
5	41	1.42	1.9	2.84	-23.9	-25.8	12
5	41	1.43	1.1	2.86	-20.0	-21.1	12
5	41	1.44	0.6	2.88	-16.3	-16.9	12
5	49	1.35	6.3	2.70	-14.8	-21.1	12
5	59	1.30	5.1	2.60	-16.1	-21.1	12
5	59	1.31	5.9	2.62	-17.3	-19.9	12
5	71	1.24	4.7	2.48	-14.5	-19.2	16
5	85	1.18	5.1	2.36	-15.3	-20.4	16
9	26	1.51	5.2	3.02	-11.3	-16.5	16
9	26	1.52	5.3	3.04	-10.9	-16.2	16

Table 4: Recurrence power range.

$R_s = R_L = 50$ ohms

Input Power = $P_{av} = V_{rms}^2 / R_L$

$V_{rms} = [P_{av}R_L]^{1/2}$

(See **Figure 3** on the schematic for measuring the input signal.)

These simulations were done with 11 harmonics.

Input Power, dBm	**Input Power, W**	**V_{rms} = $[P_{av}R_L]^{1/2}$ volt**	**V_s = $2[2]^{1/2}V_{rms}$ volt***	**Second Harmonic Power, dBc**	**Recurrence?**
-30	$1x10^{-6}$	$7.07x10^{-3}$	0.02	-60.2	yes
0	0.001	0.22	0.632	-30.7	yes
22	0.158	2.81	8.00	-17.8	yes
24.7	0.3	3.87	10.95	-9.5	no

* To obtain the desired power P_{av} we need a voltage amplitude of $[2]^{1/2}V_{rms}$. However, half the power is dissipated in R_s. In order to have P_{av} be dissipated in R_L, it is necessary to double the voltage source. Thus, the voltage amplitude should be $2[2]^{1/2}V_{rms}$.

Table 5: Expected mixing products and mixing products of inter-modulation interference.

Mixing products to look for:

* 0.008 MHz = 1.423 - 1.415
  1.407 MHz = 2.830 - 1.423
* 1.415 MHz
* 1.423 MHz
  1.431 MHz = 2.846 - 1.415
  2.822 MHz = 2.830 - 0.008
* 2.830 MHz = 2(1.415)
* 2.838 MHz = 1.415 + 1.423
* 2.846 MHz = 2(1.423)

* Expected mixing products under normal mixing circumstances.

Table 6: Inter-modulation interference and difference in powers of desired and undesired fundamentals.

Key:

n = Number of sections
P_a = Power at 1.407 MHz in dBm
P_b = Power at 1.431 MHz in dBm
P_{S1} = Power of signal 1 at 1.415 MHz in dBm
P_{S2} = Power of signal 2 at 1.423 MHz in dBm
$P_{S2} - P_{S1}$ is in dB.

n	NH	P_a	P_b	P_{S1}	P_{S2}	$P_{S2} - P_{S1}$
1	4	-182.2	-172.0	-15.9	-6.0	+9.9
13	4	-87.5	-75.8	-22.1	-11.9	+10.2
26	4	-91.0	-85.9	-23.1	-13.3	+9.8
52	4	-69.8	-48.8	-20.5	-9.1	+11.4
60	4	-63.6	-41.8	-19.6	-7.2	+12.4
70	4	-28.7	-39.6	-12.6	-7.1	+5.5
80	4	-86.7	-79.7	-23.3	-13.7	+9.6
100	4	-45.9	-19.4	-23.6	+1.9	+25.5
100	5	-27.4	-9.2	-13.0	+1.5	+14.5

ARMY RESEARCH LABORATORY
PHYSICAL SCIENCES DIRECTORATE
MANDATORY DISTRIBUTION LIST

August 1995

Defense Technical Information Center*
ATTN: DTIC-OCC
8725 John J. Kingman Rd, STE 0944
Fort Belvoir, VA 22060-6218
(*Note: Two DTIC copies will be sent from STINFO office, Ft Monmouth, NJ)

Director
US Army Material Systems Analysis Actv
ATTN: DRXSY-MP
(1) Aberdeen Proving Ground, MD 21005

Commander, AMC
ATTN: AMCDE-SC
5001 Eisenhower Ave.
(1) Alexandria, VA 22333-0001

Director
Army Research Laboratory
ATTN: AMSRL-D (John W. Lyons)
2800 Powder Mill Road
(1) Adelphi, MD 20783-1197

Director
Army Research Laboratory
ATTN: AMSRL-DD (COL Thomas A. Dunn)
2800 Powder Mill Road
(1) Adelphi, MD 20783-1197

Director
Army Research Laboratory
2800 Powder Mill Road
Adelphi, MD 20783-1197
(1) AMSRL-OP-SD-TA (ARL Records Mgt)
(1) AMSRL-OP-SD-TL (ARL Tech Library)
(1) AMSRL-OP-SD-TP (ARL Tech Publ Br)

Directorate Executive
Army Research Laboratory
Physical Sciences Directorate
Fort Monmouth, NJ 07703-5601
(1) AMSRL-PS
(1) AMSRL-PS-T (M. Hayes)
(1) AMSRL-OP-FM-RM
(22) Originating Office

Advisory Group on Electron Devices
ATTN: Documents
Crystal Square 4
1745 Jefferson Davis Highway, Suite 500
(2) Arlington, VA 22202

Commander, CECOM
R&D Technical Library
Fort Monmouth, NJ 07703-5703
(1) AMSEL-IM-BM-I-L-R (Tech Library)
(3) AMSEL-IM-BM-I-L-R (STINFO Ofc)

ARMY RESEARCH LABORATORY
PHYSICAL SCIENCES DIRECTORATE
SUPPLEMENTAL DISTRIBUTION LIST
(ELECTIVE)

Deputy for Science & Technology
Office, Asst Sec Army (R&D)
(1) Washington, DC 20310

HQDA (DAMA-ARZ-D/
Dr. F.D. Verderame)
(1) Washington, DC 20310

Director
Naval Research Laboratory
ATTN: Code 2627
(1) Washington, DC 20375-5000

USAF Rome Laboratory
Technical Library, FL2810
ATTN: Documents Library
Corridor W, STE 262, RL/SUL
26 Electronics Parkway, Bldg 106
Griffiss Air Force Base
(1) NY 13441-4514

Dir, ARL Battlefield
Environment Directorate
ATTN: AMSRL-BE
White Sands Missile Range
(1) NM 88002-5501

Dir, ARL Sensors, Signatures,
Signal & Information Processing
Directorate (S3I)
ATTN: AMSRL-SS
2800 Powder Mill Road
(1) Adelphi, MD 20783-1197

Dir, CECOM Night Vision/
Electronic Sensors Directorate
ATTN: AMSEL-RD-NV-D
(1) Fort Belvoir, VA 22060-5806

Dir, CECOM Intelligence and
Electronic Warfare Directorate
ATTN: AMSEL-RD-IEW-D
Vint Hill Farms Station
(1) Warrenton, VA 22186-5100

Cdr, Marine Corps Liaison Office
ATTN: AMSEL-LN-MC
(1) Fort Monmouth, NJ 07703-5033